BRAIN COMMUNICATIONS

Prediction of conversion to Alzheimer's disease using deep survival analysis of MRI images

Tomonori Nakagawa,[1] Manabu Ishida,[2,3] Junpei Naito,[3] Atsushi Nagai,[2] Shuhei Yamaguchi[2] and Keiichi Onoda[2,4], on behalf of the Alzheimer's Disease Neuroimaging Initiative[+]

[+]Data used in this article were obtained in part from the Alzheimer's Disease Neuroimaging Initiative (ADNI) database (adni.loni.usc.edu). As such, the investigators within the ADNI contributed to the design and implementation of ADNI and/or provided data but did not participate in analysis or writing of this article. A complete listing of ADNI investigators can be found at: adni. loni. usc. edu/ wp-content/ uploads/ how_ to_ apply/ ADNI_ Acknowledgement_ List. pdf.

The prediction of the conversion of healthy individuals and those with mild cognitive impairment to the status of active Alzheimer's disease is a challenging task. Recently, a survival analysis based upon deep learning was developed to enable predictions regarding the timing of an event in a dataset containing censored data. Here, we investigated whether a deep survival analysis could similarly predict the conversion to Alzheimer's disease. We selected individuals with mild cognitive impairment and cognitively normal subjects and used the grey matter volumes of brain regions in these subjects as predictive features. We then compared the prediction performances of the traditional standard Cox proportional-hazard model, the DeepHit model and our deep survival model based on a Weibull distribution. Our model achieved a maximum concordance index of 0.835, which was higher than that yielded by the Cox model and comparable to that of the DeepHit model. To our best knowledge, this is the first report to describe the application of a deep survival model to brain magnetic resonance imaging data. Our results demonstrate that this type of analysis could successfully predict the time of an individual's conversion to Alzheimer's disease.

1 Department of Neurology, Masuda Red Cross Hospital, Masuda 698-8501, Japan
2 Department of Neurology, Shimane University, Izumo 693-8501, Japan
3 ERISA Corporation, Matsue 690-0816, Japan
4 Department of Psychology, Otemon Gakuin University, Osaka 567-8502, Japan

Correspondence to: Keiichi Onoda, PhD
Department of Psychology, Otemon Gakuin University
2-1-15 Nishiai, Ibaraki City, Osaka 567-8502, Japan
E-mail: onodak1@gmail.com

Keywords: Alzheimer's disease; mild cognitive impairment; prediction of conversion; deep survival analysis

Abbreviations: AAL = automated anatomical labelling; BNA = Brainnetome Atlas; GMV = grey matter volume; MCI = mild cognitive impairment; MMSE = mini-mental state examination; NC = normal control; ROI = region of interest

Received January 16, 2020. Revised March 18, 2020. Accepted April 15, 2020. Advance Access publication May 12, 2020

Graphical Abstract

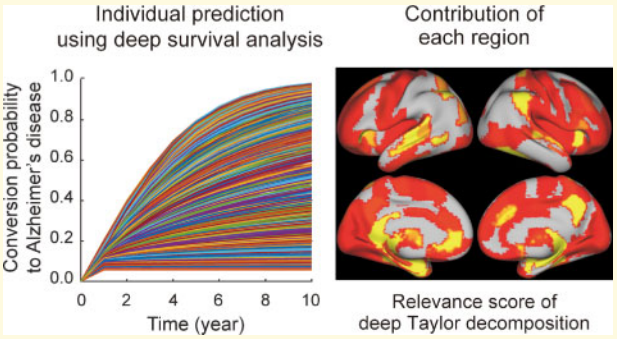

Introduction

Alzheimer's disease, a progressive neurodegenerative disorder, is the most common cause of dementia in late life (Breteler *et al.*, 1992). Alzheimer's disease causes neuronal death and tissue loss throughout the brain (Jack *et al.*, 1997). Consequently, patients usually undergo progressive stages of cognitive and memory impairment, including the prodromal stage of Alzheimer's disease, which is characterized by mild cognitive impairment (MCI). Approximately 10–15% of patients with MCI develop Alzheimer's disease annually (Petersen *et al.*, 2009), and currently, there is no cure or method to reverse the progression of disease. Therefore, computer-aided systems that can enable an early and accurate prediction of the onset and classification of the prodromal stage are essential for the intervention and prevention of Alzheimer's disease progression (Bron *et al.*, 2015).

Previous studies have explored MRI biomarkers of Alzheimer's disease, including brain atrophy. In particular, high-dimensional MRI pattern classification methods have been shown to identify Alzheimer's disease and MCI with a high degree of reliability (Arbabshirani *et al.*, 2017). Many studies have used support vector machines, a representative method of machine learning (Magnin *et al.*, 2009; Davatzikos *et al.*, 2011; Khedher *et al.*, 2015; Moradi *et al.*, 2015; Retico *et al.*, 2015). Another promising approach involves deep learning, a modern branch of machine learning inspired by human neural networks (Jo *et al.*, 2019). This latter approach, which was developed using complicated algorithms to model high-level features, can extract abstractions from datasets (LeCun *et al.*, 2015). Therefore, deep learning is advantageous in terms of automatic feature selection, even though the learning cost is high when compared to other approaches. For example, previous studies designed fine deep learning techniques based on convolutional neural networks to classify progressive and stable MCI using MRI data (Lin *et al.*, 2018; Spasov *et al.*, 2019). These methods achieved accuracies of 0.79–0.86 in cross-validation studies. Apparently, such machine learning approaches have successfully classified clinical groups, including Alzheimer's disease patients versus normal controls (NC), MCI patients versus NC and progressive MCI versus stable MCI patients (Arbabshirani *et al.*, 2017). However, certain important issues remain to be addressed.

One such issue involves the prediction of the timing when an individual with MCI or a normal individual will convert to Alzheimer's disease. As described above, certain patients with MCI convert to Alzheimer's disease, whereas others remain in the MCI stage. Therefore, it is important to predict the group of MCI subjects who would convert to Alzheimer's disease in the future (Zhang and Shen, 2012). Previous studies that used machine learning approaches to classify MCI subjects as Alzheimer's disease converters and non-converters have reported moderate levels of accuracy (66.0–80.9%) (Arbabshirani *et al.*, 2017). To our knowledge, all previous research (Arbabshirani *et al.*, 2017) concerning Alzheimer's disease conversion has focused on the prediction of converters and non-converters to Alzheimer's disease within a 2- or 3-year period. This approach raises two issues. First, available medical datasets always include censored data. In this case, the censored data are information from subjects who were lost to follow-up before conversion was detected. Previous studies used only subjects that had completed a 2- or 3-year follow-up assessment, implying the exclusion of censored data. Moreover, the observation that the censored subjects were healthy until the censored time point is also important. Second, it is necessary to forecast whether a subject would convert to Alzheimer's disease within 2 or 3 years, and when, specifically, the conversion would occur. Therefore, a survival analysis is more suitable for such databases.

A survival analysis is an analysis of time-to-event data, which describe the interval between a time origin to an endpoint of interest (Kartsonaki, 2016). A recently developed approach that combines survival analysis and deep learning enables the estimation of the survival durations of individual patients (Liao and Hyung-il, 2016;

Ranganath *et al.*, 2016; Luck and Lodi, 2017; Chaudhary *et al.*, 2018; Huang *et al.*, 2018; Katzman *et al.*, 2018). For instance, Ranganath *et al.* (2016) introduced the deep survival analysis, a hierarchical generative approach to a survival analysis in the context of electronic health records. The analysis uses a Weibull distribution, which is popular for survival analyses, to model the time of an event. Ranganath *et al.* (2016) reported that the deep survival analysis yielded a more accurate stratification of patients based on the risk of developing coronary heart disease. Furthermore, Katzman *et al.* (2018) introduced a Cox proportional hazards-based deep neural network for modelling the interactions between a patient's covariates and treatment effectiveness, with the intent to provide personalized treatment recommendations. The authors demonstrated that this approach successfully modelled complex relationships between a patient's covariates and the risk of failure. Both studies suggested that a survival analysis based on deep learning could predict an individual's risk of developing diseases, as well as possible interventions. In this study, we introduced a deep learning method-based survival analysis to estimate the probability that an individual would progress to Alzheimer's disease in a given period of time.

Materials and methods

Subjects

This study included individuals from the following cohorts: Alzheimer's Disease Neuroimaging Initiative, Australian Imaging, Biomarkers and Lifestyle Flagship Study of Ageing, Japanese Alzheimer's Disease Neuroimaging Initiative and our hospital patients. Data collection was conducted according to the relevant regulations of each centre (see Supplementary material for details). All participants provided written consent to participate, according to the Declaration of Helsinki. Approval for the study was obtained from the local ethics committees.

The subjects in the current study were selected from among patients with diagnosed MCI and NCs at baseline. This selection was also based on the availability of magnetization prepared rapid gradient echo images. The follow-up interval was estimated as the difference between the date of the baseline MRI measurement and the diagnosis at follow-up. The subjects' data are summarized in Tables 1 and 2. Briefly, we collected the data of 2142 subjects, of whom a quarter converted to Alzheimer's disease. The mean intervals of conversion in each database ranged from 1.4 to 2.6 years. Those who converted to Alzheimer's disease were older than non-converters and had lower mini–mental state examination (MMSE) scores.

Structural image pre-processing

The pre-processing of T_1-weighted images was performed using statistical parametric mapping and the computational anatomy toolbox on the MATLAB platform (MathWorks, Natick, MA, USA). All images were spatially normalized and segmented into grey matter, white matter and cerebrospinal fluid. The voxel size was 27 mm^3.

We extracted the grey matter volume (GMV) of each region of interest (ROI) based on two atlases (Fig. 1A): the automated anatomical labelling (AAL), which is frequently used in the field of neuroimaging and consists of 116 regions, and the Brainnetome Atlas (BNA) (Fan *et al.*, 2016), which contains 246 subregions. We calculated the mean values of the ROIs for each individual (Fig. 2A). The analysis was conducted for both atlases (AAL and BNA).

Feature

The mean GMVs of regions based on the AAL or BNA were treated as input features for the survival models. Recently, certain imaging studies demonstrated that clinical information could improve the accuracy of a prediction of conversion to Alzheimer's disease (Blazhenets *et al.*, 2019; Zhou *et al.*, 2019). Therefore, we also investigated whether clinical information could improve the performance of a survival analysis. Here, we included the age and MMSE score, which were available for every individual regardless of the database. Therefore, we set three patterns: GMV, GMV + age and GMV + Age + MMSE.

Our deep survival model

The analysis procedure is summarized in Fig. 1B–D. We treated the follow-up intervals as discrete values to yield a time set of $t = 0, 1, \ldots, T$. T was set as 12 in the current study because the maxima of the follow-up interval, $i \in t$, was the time when the event or censoring occurred. We defined e as the conversion to Alzheimer's disease (0: censored, 1: uncensored). Therefore, each data point (i.e. subject) contained three numbers (x, i, e), where $x \in X$ is a n-dimensional covariate ($n = 116$ in case of GMV of AAL). We were interested in the true probability $P(t|x)$ for each tuple.

We developed a deep neural network model to compute the time course of an event, which in this case was the conversion to Alzheimer's disease. The model took x as the input. The second to fourth layers consisted of 32 units with the rectified linear unit activation. L1 and L2 regularizations penalized the weights in each layer, and a dropout rate of 50% was applied to these layers. The fifth layer consisted of two single units (m, s), which were the parameters of the cumulative Weibull distribution $[1 - \exp(-t^m/s)]$. These parameters (m, s) decided the shape and scale of the distribution. The activation functions of the Weibull distribution parameter layer

Table 1 Characteristics of the study subjects

	ADNI	AIBL	JADNI	Shimane	All
n	1366	257	419	100	2142
MCI/NC	846/520	49/208	259/160	57/43	1211/931
Age, MCI (years)	72.9 ± 7.7	76.0 ± 7.0	72.9 ± 5.9	76.6 ± 6.9	73.3 ± 7.4
NC	74.9 ± 6.1	72.1 ± 6.9	67.9 ± 5.7	70.3 ± 4.5	72.8 ± 6.6
Sex (F/M) (%)	44.7/55.3	50.2/49.8	50.1/49.9	53.0/47.0	53.2/46.8
MMSE MCI	27.5 ± 1.8	27.2 ± 2.1	26.4 ± 1.7	25.6 ± 2.5	27.2 ± 1.9
NC	29.1 ± 1.1	28.8 ± 1.2	29.2 ± 1.2	29.1 ± 1.2	29.0 ± 1.1
Conversion (*n*)	378	30	104	20	532
MCI/NC	352/26	25/5	104/0	20/0	501/31
Mean interval (years)	3.9	3.8	2.5	2.3	3.5
MRI (%) (1.5/3.0 T)	43.9/56.2	35.0/65.0	88.5/11.5	93.0/7.0	53.8/46.2

ADNI = Alzheimer's Disease Neuroimaging Initiative; AIBL = Australian Imaging, Biomarkers and Lifestyle Flagship Study of Ageing; F = female; JADNI = Japanese Alzheimer's Disease Neuroimaging Initiative; M = male.

Table 2 Comparison between converters to Alzheimer's disease and non-converters

	ADNI	AIBL	JADNI	Shimane	All
N					
Converter	378	30	104	20	532
Non-converter	988	227	315	80	1610
Age (years)					
Converter	73.8 ± 7.3	76.6 ± 7.0[a]	73.6 ± 5.6[a]	79.2 ± 4.1[a]	74.1 ± 7.0[a]
Non-converter	73.6 ± 7.1	72.3 ± 7.0	70.1 ± 6.3	72.6 ± 6.6	72.7 ± 7.0
Female gender (%)					
Converter	39.7[a]	50.0	62.5[a]	55.0	45.3
Non-converter	46.6	50.2	46.0	52.0	42.3
MMSE					
Converter	27.1 ± 1.8[a]	27.2 ± 2.1[a]	25.8 ± 1.5[a]	25.7 ± 2.7[a]	26.8 ± 1.9[a]
Non-converter	28.5 ± 1.6	28.6 ± 1.4	28.0 ± 2.0	27.5 ± 2.6	28.4 ± 1.7
Interval					
Converter	2.6 ± 2.2[a]	2.4 ± 1.3[a]	1.6 ± 0.6[a]	1.4 ± 1.2[a]	2.4 ± 2.0[a]
Non-converter	4.4 ± 2.9	4.0 ± 1.1	2.8 ± 0.6	2.6 ± 2.1	3.9 ± 2.4

[a]A significant difference between converters and non-converters.
ADNI = Alzheimer's Disease Neuroimaging Initiative; AIBL = Australian Imaging, Biomarkers and Lifestyle Flagship Study of Ageing; JADNI = Japanese Alzheimer's Disease Neuroimaging Initiative.

used soft plus and rectified linear unit for m and s, respectively. The conversion ratio was then computed and stored in the final layer using these parameters. The final layer contained T units, and the output value at the index, t, corresponded to the probability of conversion at t years. This model is shown in Fig. 1B.

To train our model, we minimized the loss function, L, which was designed to handle censored data. This function captured both the event and the time when the event occurred in subjects who were not censored. Conversely, it captured the time of censoring in censored subjects and thus provided the information available for the subject at that time. We defined L using the following formula:

$$L = -\sum_{n=1}^{N}\left[\mathrm{f(e=1)}\sum_{t=1}^{T}(P_{t,n}-C_{t,n})^2 + \mathrm{f(e=0)}\sum_{t=1}^{i_n}(P_{t,n}-C_{t,n})^2\right],$$

where f(e) is an indicator function and $C_{t,n}$ indicates whether the subject n had Alzheimer's disease (1) or not (0) at time t. The indicator function f(e = 1) takes the value 1 when the event happens and the value 0 when the event does not happen, whereas f(e = 0) takes the value 0 when the event happens and the value 1 when the event does not happen. The first term captures the information provided by the uncensored subjects, whereas the second term captures the censoring bias by exploiting the knowledge that the subjects did not have Alzheimer's disease at that time. In Fig. 1C, we have illustrated a frame used to compute the training loss of our deep survival network. For converters, C is 0 at all times before first Alzheimer's disease diagnosis and 1 after that. For non-converters, C is 0 until the last follow-up examination and the subsequence indeterminate information is not considered in the model. The Adam optimizer was used as a default setting, with a batch number of 128 and a maximum training epoch number of 200. Early stopping was applied when the validation loss did not improve over a period of longer than 10 epochs.

The data were partitioned randomly into three sets: a training set with 80%, a validation set with 10% and a test set with 10%. The model was trained using a

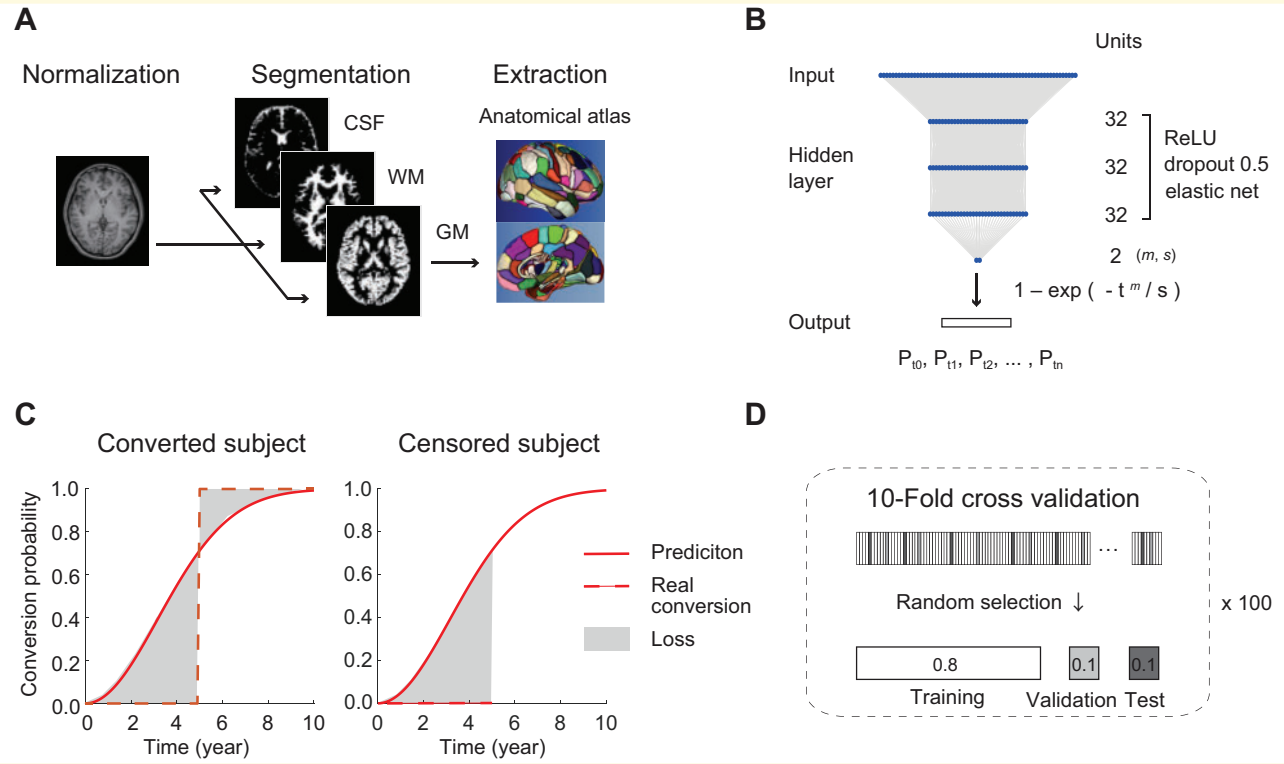

Figure 1 Overview of the analysis. (**A**) Pre-processing of MRI images including normalization, segmentation and extraction of the grey matter volume based on the anatomical atlas. (**B**) Deep survival model consisting of the input layer, three hidden layers, a parametric layer of the cumulative Weibull distribution and an output layer. (**C**) Concept of the loss function. Left, the case of an uncensored (converted) subject; right, the case of a censored subject. (**D**) Analysis procedure based on 10 cross fold validations. ReLu = rectified linear unit.

maximum of 200 epochs, and the best performing model with the lowest loss in the validation set was saved. The model's performance was then evaluated in the test set. We repeated this procedure 100 times for every model and input feature (Fig. 1D).

Model comparison

We compared three models: the Cox proportional hazards model, DeepHit (Lee *et al.*, 2018) and our model. The Cox proportional hazards model is a standard survival analysis. This model assumes that a subject's risk of event is a linear combination of the patient's covariates. In contrast to models with strong parametric assumptions, DeepHit uses a deep neural network to learn the distribution of survival times directly without assumptions about the underlying stochastic process. Thus, this model allows for the possibility of a change over time in the relationship between covariates and risk.

A concordance index was used to evaluate the performance of the three models. This index is a standard measure used to estimate the efficiency of a model for ranking survival times by calculating the probability that the event times of causes taken in pairs will be ranked correctly (see Supplementary material). The concordance index was averaged over time (1–10 years).

Statistical analysis

To compare the concordance indices between the models, two-tailed *t*-tests were conducted. The *P*-values were corrected using the Bonferroni method to control Type I errors.

Contribution of each region

We used a deep Taylor decomposition (Montavon *et al.*, 2017), which decomposes the model prediction into the contributions of its input elements, to assess the importance of single ROIs in the prediction of Alzheimer's disease conversion (see Supplementary material). We computed and averaged the relevance scores for the ROI data in each individual. The ROI-level significance was assessed using a permutation test that created a null distribution by repeating the prediction with a randomized conversion label and interval of 100 times.

Data availability

Alzheimer's Disease Neuroimaging Initiative (http:// adni. loni. usc. edu/), Australian Imaging, Biomarkers and Lifestyle Flagship Study of Ageing (https:// aibl. csiro. au/) and Japanese Alzheimer's Disease Neuroimaging Initiative (https:// humandbs. biosciencedbc. jp/ en/ hum0043-v1)

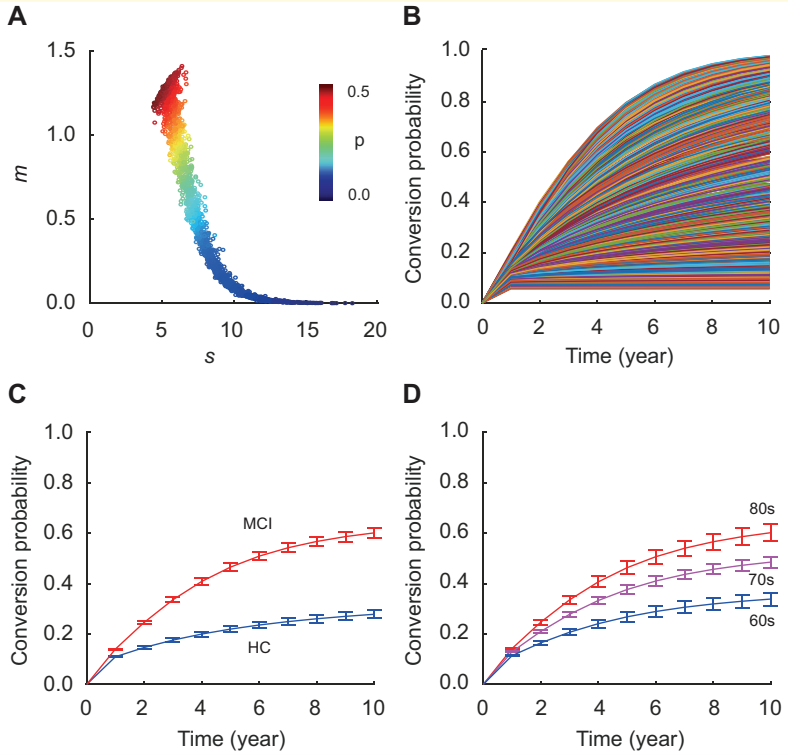

Figure 2 Intermediate parameters and conversion curves of our deep survival model. (**A**) Estimated parameters of the cumulative Weibull distribution [$1 - \exp(-t^m/s)$] as computed by our deep survival model. The variables m and s refer to shape and scale parameters, respectively. Each point indicates an individual subject, and the colour reflects their probability of conversion within 3 years. The graph indicates a higher risk of conversion to Alzheimer's disease (higher m) at an earlier time (smaller s). (**B**) Superimposed plots of the estimated probability curves for the conversion to Alzheimer's disease in all subjects. (**C**) Mean estimated probability curves for the MCI and NC groups. (**D**) Mean estimated probability curves for patients aged 60–69, 70–79 and 80–89 years. Error bars of in **C** and **D** denote the 95% confidence intervals.

data are available publicly via the indicated websites. We have also made the input features (GMV of each ROI and demographics) and analysis script of our model available to the public (github.com/onodak1/demo).

Results

First, we extracted the intermediate parameters (m, s) of our deep survival models using GMV data of the BNA for the test sets and averaged these parameters in each individual. The distribution of parameters is illustrated in Fig. 2A. As shown in the figure, a subject with a lower s and a higher m has a higher risk of converting to Alzheimer's disease at an earlier time point, whereas a subject with a higher s and a lower m has a lower risk of conversion. The distribution of parameters along the curve is a function of the risk of conversion. We superimposed all individual curves of the predicted conversion probabilities as a function of the follow-up years in Fig. 2B. To evaluate the effects of group and age on the probability of Alzheimer's disease conversion, we computed the mean estimated probability of the MCI/NC groups or age groups (60–69, 70–79 and 80–89 years) in each study year. The estimated probability of Alzheimer's disease conversion was noticeably higher for the MCI group than for the NC group (Fig. 2C), and the timewise change in the MCI group was consistent with a previous report that the typical rate of conversion to Alzheimer's disease in this group is 10–15% per year (Petersen *et al.*, 2009). In terms of age, the estimated conversion ratio was higher for older patients (Fig. 2D).

Figure 3 presents the concordance indices calculated in this study. The datasets comprised 12 patterns, including the atlas (AAL or BNA), feature (GMV, GMV + Age, or GMV + Age + MMSE) and group (both MCI/NC or only MCI). We applied three models, the traditional standard Cox proportional-hazard model, DeepHit and our model, to each dataset. The concordance index distributions were 0.78–0.83 for the MCI/NC set and 0.69–0.75 for the MCI set. Overall, the two deep learning models yielded higher concordance indices when compared with the Cox model. Particularly, for BNA, the differences between the deep learning and Cox models were significant ($ts(198) > 5.3$, $Ps < 10^{-6}$). To examine whether clinical information would improve the prediction performance, we added the individual's age and MMSE score as features. The addition of

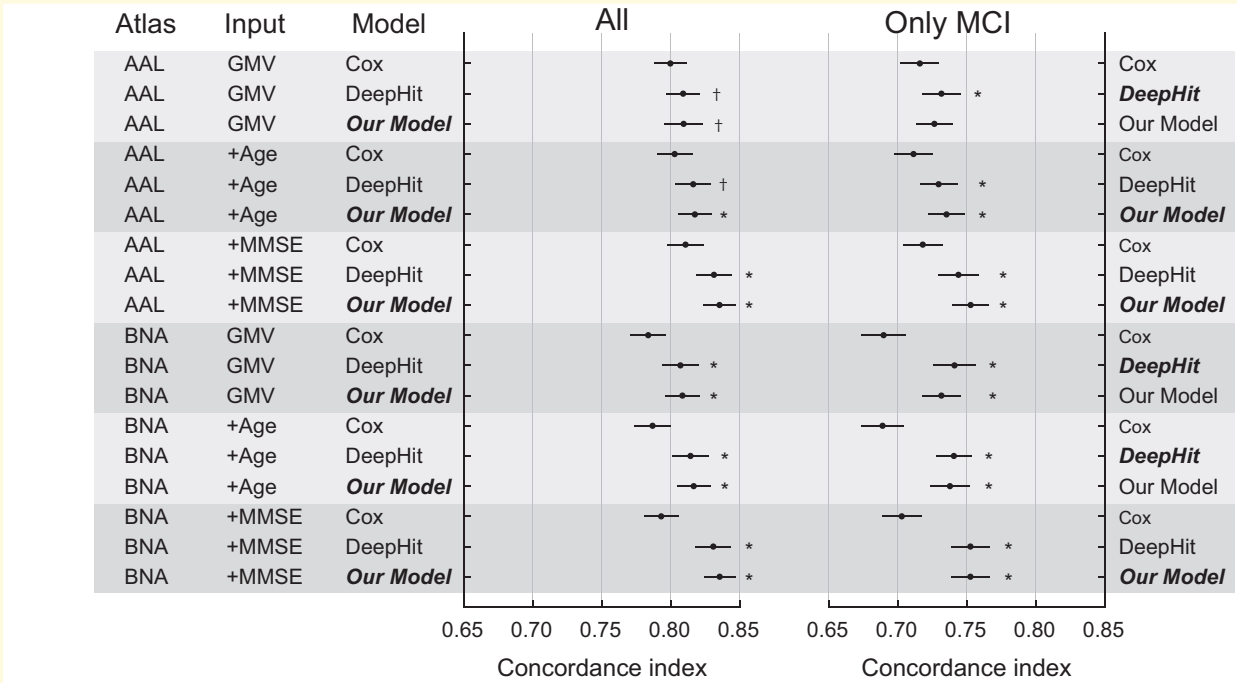

Figure 3 Comparisons of concordance indices estimated in the Cox proportional-hazard, DeepHit and our deep survival models. The circles and error bars depict the means and 95% confidence intervals, respectively. Italics and bold type indicate the best model among the three options. *Bonferroni-corrected $P < 0.05$ and †uncorrected $P < 0.05$ indicate a significantly higher concordance index relative to the Cox model.

both variables improved the concordance indices in all cases. Particularly in the MCI/NC set, the concordance indices were significantly higher for the two deep learning models that included age and MMSE than for the models without those variables ($ts(198) > 5.3$, $Ps < 10^{-6}$). In the MCI set, our deep survival models that included age and MMSE yielded higher concordance indices than those in which only GMV was included, for both atlases ($ts(198) > 4.1$, $Ps < 10^{-4}$). In contrast, the addition of age alone did not significantly improve the concordance indices in every condition. Eventually, our deep survival model that included the GMV, age and MMSE yielded maximum concordance indices of 0.835 and 0.753 for the MCI/NC and MCI sets, respectively.

Figure 4 depicts the contribution of each ROI based on AAL and BNA in our deep survival model, which was computed as a relevance score of deep Taylor decomposition. The relevance scores of the inferior parietal cortex, lateral and medial temporal cortex, cingulate cortex, insula and thalamus are higher than those of other regions. This result indicates that our deep survival model estimated the conversion probability to Alzheimer's disease based on information from these regions.

Discussion

In this study, we used a deep survival analysis to predict the progression to Alzheimer's disease from existing data. This approach appeared to perform better than the standard Cox proportional-hazard model and comparably to the existing deep learning model, DeepHit. Both deep survival models enabled an estimation of the probability that an individual subject would convert to Alzheimer's disease within a given time period.

Brain atrophy, as assessed by MRI, has been used conventionally to predict the conversion to Alzheimer's disease. Certain reviews (Arbabshirani *et al.*, 2017; Leandrou *et al.*, 2018) and articles describing experimental studies (Costafreda *et al.*, 2011; Eskildsen *et al.*, 2013; Lin *et al.*, 2018) have summarized previous research that aimed to predict progression to Alzheimer's disease. Those reviews suggested that brain atrophy measures could classify converters and non-converters with accuracy levels ranging between 0.6 and 0.9. Moreover, the accuracy of classification decreased as the sample size increased (Leandrou *et al.*, 2018). All previous studies essentially divided MCI subjects into two groups: converters or non-converters within 2 or 3 years. Therefore, censored data were not considered when predicting the conversion to Alzheimer's disease. As a survival analysis model is effective for censored data, our deep survival analysis model based on big data achieved a concordance index of 0.75 when using only MCI.

The deep survival analysis was first introduced by Faraggi and Simon (1995), who developed an expanded Cox proportional hazards model with a neural network

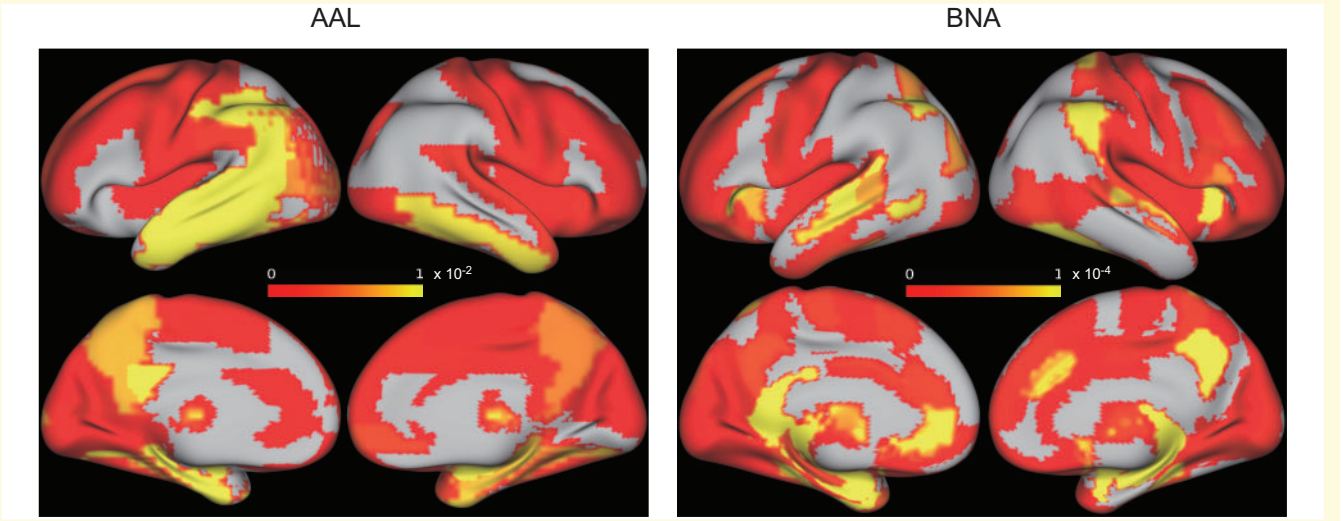

Figure 4 Contribution of each region as calculated using a deep Taylor decomposition. Region separation was based on AAL (left panel) or the BNA (right panel). Coloured areas indicate regions with significantly higher relevance score compared to the null distribution.

structure. Thereafter, other groups developed different approaches to the deep survival analysis (Ranganath *et al.*, 2016; Luck and Lodi, 2017; Chaudhary *et al.*, 2018; Huang *et al.*, 2018; Katzman *et al.*, 2018). In this study, we compared our model with DeepHit, a deep learning model that lacks any strong assumptions and can directly estimate the probability in each year. This model achieved much better performances for medical data than other previous models (Lee *et al.*, 2018). Our deep survival model based on a Weibull distribution reached a performance level nearly equal to that of DeepHit and thus has a sufficient ability to predict a medical event. The most important difference between DeepHit and our model is that our model assumes the temporal distribution of event timing. Alzheimer's disease is an irreversible disease because of the gradual neurodegeneration and the lack of effective treatment. Therefore, assuming a gradual increase of conversion risk with ageing would be natural.

At an individual level, a survival analysis has an advantage in clinical settings because it allows the classification of converters and non-converters within a given number of years and can also identify early and late converters. Several recent attempts have been made to classify early and late Alzheimer's disease converters (Li *et al.*, 2018; Shen *et al.*, 2018), and these have yielded reasonably high levels of accuracy (0.92–0.93). Therefore, our approach might require further refinement to increase the accuracy of short-term predictions of the progression from MCI to Alzheimer's disease.

When predicting Alzheimer's disease conversion from MRI images, the addition of clinical information can improve the performance. Previous studies have demonstrated that Cox models based on imaging and clinical variables exhibited superior predictive and diagnostic value when compared to models based on only imaging data (Blazhenets *et al.*, 2019; Zhou *et al.*, 2019). In this study, we included the age and MMSE score as features and compared the prediction performances of models with and without these clinical variables. As in previous reports, we observed robust improvements in the prediction performances when both age and MMSE were added, whereas age alone had no significant effect. A loss of GMV is strongly correlated with age (Ge *et al.*, 2002) and can predict age with high accuracy ($r = 0.92$ between the estimated and real ages) (Franke *et al.*, 2010), suggesting that the GMV in each region contains rich information that reflects the chronological age.

A recent expansion of deep learning methodology has enabled an understanding of the part of the input on which the model focuses. In this study, the deep Taylor decomposition analysis revealed that the inferior parietal cortex, lateral and medial temporal cortex, cingulate cortex, insula and thalamus especially contributed to the prediction of Alzheimer's disease conversion. These regions are equivalent to the default mode and salience network (Damoiseaux *et al.*, 2006; Seeley *et al.*, 2007) and most correspond with regions exhibiting hypometabolism and amyloid plaque accumulation (Buckner *et al.*, 2008; Palop and Mucke, 2010). These observed regions were repeatedly identified in previous voxel-based morphometry studies for Alzheimer's disease and MCI (Mueller *et al.*, 2012; Minkova *et al.*, 2017). Furthermore, a classification study of MCI based on support vector machine suggested the heavy weighting of similar regions in their model (Aguilar *et al.*, 2013). In other words, both prediction and classification models might focus on information about similar regions and detect similar patterns of

atrophy, albeit each model is tailored for the specific purpose. Possibly, we may be able to detect a slight distribution of brain atrophy suggestive of later Alzheimer's disease conversion, especially when using the default mode network. This is particularly relevant in the case of Alzheimer's disease conversion.

One limitation of this study was our lack of consideration of competing risks or the possibility that a subject might convert to another type of dementia, such as dementia with Lewy bodies or frontotemporal dementia. Recently, deep learning has been used to develop a multi-task model of survival analysis with competing risks (Lee *et al.*, 2018), in which the model directly learns the joint distributions of survival times and events. The application of this type of multi-task model to dementia studies would be useful. However, public databases that include MRI images of patients with dementia with Lewy bodies or frontotemporal dementia are currently unavailable. Therefore, it will be necessary to develop databases that include structural images of the subjects during the pre-dementia stage, as well as the final diagnosis of the dementia subtype. Furthermore, we must consider recent changes in research regarding the diagnosis of Alzheimer's disease using ATN staging (Jack *et al.*, 2018). In this framework, biomarkers are grouped into β amyloid deposition, pathologic tau and neurodegeneration. This new framework could improve the accuracy of prediction of conversion to Alzheimer's disease. We conducted additional sub-group analyses for the subjects who underwent amyloid PET measurements and confirmed that amyloid PET quantification improved the prediction performance (see Supplementary material). However, we could not conduct the analyses for only NC group due to the small number of Alzheimer's disease converters. To establish the long-term prediction of Alzheimer's disease conversion, more cases need to be assessed.

In conclusion, structural changes can be detected by MRI even 10 years before a clinical diagnosis of Alzheimer's disease (Tondelli *et al.*, 2012). Here, we demonstrated that a deep survival analysis could predict the timing of conversion to Alzheimer's disease at an individual level, with good accuracy. We have identified some specific remaining issues, including the need to make more precise predictions, especially with respect to very short-term predictions and differential diagnoses of other dementia types. However, we expect that our results will yield a significant contribution to clinical trials with respect to predicting the conversion to Alzheimer's disease, the most prevalent type of dementia.

Supplementary material

Supplementary material is available at *Brain Communications* online.

Funding

This research was supported by the program for Impulsing Paradigm Change through Disruptive Technologies (ImPACT) of Council for Science, Technology and Innovation (Cabinet Office, Government of Japan).

Competing interests

The authors report no competing interests.

References

Aguilar C, Westman E, Muehlboeck JS, Mecocci P, Vellas B, Tsolaki M, et al. Different multivariate techniques for automated classification of MRI data in Alzheimer's disease and mild cognitive impairment. Psychiatry Res 2013; 212: 89–98.

Arbabshirani MR, Plis S, Sui J, Calhoun VD. Single subject prediction of brain disorders in neuroimaging: promises and pitfalls. Neuroimage 2017; 145: 137–65.

Blazhenets G, Ma Y, Sörensen A, Rücker G, Schiller F, Eidelberg D, et al Principal components analysis of brain metabolism predicts development of Alzheimer dementia. J Nucl Med 2019; 60: 837–43.

Breteler MM, Claus JJ, van Duijn CM, Launer LJ, Hofman A. Epidemiology of Alzheimer's disease. Epidemiol Rev 1992; 14: 59–82.

Bron EE, Smits M, van der Flier WM, Vrenken H, Barkhof F, Scheltens P, et al. Standardized evaluation of algorithms for computer-aided diagnosis of dementia based on structural MRI: the CADDementia challenge. Neuroimage 2015; 111: 562–79.

Buckner RL, Andrews-Hanna JR, Schacter DL. The brain's default network: anatomy, function, and relevance to disease. Ann N Y Acad Sci 2008; 1124: 1–38.

Chaudhary K, Poirion OB, Lu L, Garmire LX. Deep learning-based multi-omics integration robustly predicts survival in liver cancer. Clin Cancer Res 2018; 24: 1248–59.

Costafreda SG, Dinov ID, Tu Z, Shi Y, Liu CY, Kloszewska I, et al. Automated hippocampal shape analysis predicts the onset of dementia in mild cognitive impairment. Neuroimage 2011; 56: 212–9.

Damoiseaux JS, Rombouts S, Barkhof F, Scheltens P, Stam CJ, Smith SM, et al. Consistent resting-state networks across healthy subjects. Proc Natl Acad Sci USA 2006; 103: 13848–53.

Davatzikos C, Bhatt P, Shaw LM, Batmanghelich KN, Trojanowski JQ. Prediction of MCI to AD conversion, via MRI, CSF biomarkers, and pattern classification. Neurobiol Aging 2011; 32: 2322.e19–27.

Eskildsen SF, Coupé P, García-Lorenzo D, Fonov V, Pruessner JC, Collins DL. Prediction of Alzheimer's disease in subjects with mild cognitive impairment from the ADNI cohort using patterns of cortical thinning. Neuroimage 2013; 65: 511–21.

Fan L, Li H, Zhuo J, Zhang Y, Wang J, Chen L, et al. The human Brainnetome Atlas: a new brain atlas based on connectional architecture. Cereb Cortex 2016; 26: 3508–26.

Faraggi D, Simon R. A neural network model for survival data. Stat Med 1995; 14: 73–82.

Franke K, Ziegler G, Klöppel S, Gaser C. Alzheimer's Disease Neuroimaging Initiative. Estimating the age of healthy subjects from T1-weighted MRI scans using kernel methods: exploring the influence of various parameters. Neuroimage 2010; 50: 883–92.

Ge Y, Grossman RI, Babb JS, Rabin ML, Mannon LJ, Kolson DL. Age-related total gray matter and white matter changes in normal adult brain. Part I: volumetric MR imaging analysis. AJNR Am J Neuroradiol 2002; 23: 1327–33.

Huang C, Zhang A, Xiao G. Deep integrative analysis for survival prediction. Pac Symp Biocomput 2018; 23: 343–52.

Jack CR Jr, Bennett DA, Blennow K, Carrillo MC, Dunn B, Haeberlein SB, et al. NIA-AA research framework: toward a biological definition of Alzheimer's disease. Alzheimers Dement 2018; 14: 535–62.

Jack CR, Petersen RC, Xu YC, Waring SC, O'Brien PC, Tangalos EG, et al. Medial temporal atrophy on MRI in normal aging and very mild Alzheimer's disease. Neurology 1997; 49: 786–94.

Jo T, Nho K, Saykin AJ. Deep learning in Alzheimer's disease: diagnostic classification and prognostic prediction using neuroimaging data. Front Aging Neurosci 2019; 11: 20.

Kartsonaki C. Survival analysis. Diagn Histopathol 2016; 22: 263–70.

Katzman JL, Shaham U, Cloninger A, Bates J, Jiang T, Kluger Y. DeepSurv: personalized treatment recommender system using a Cox proportional hazards deep neural network. BMC Med Res Methodol 2018; 18: 24.

Khedher L, Ramírez J, Górriz JM, Brahim A, Segovia F. Early diagnosis of Alzheimer's disease based on partial least squares, principal component analysis and support vector machine using segmented MRI images. Neurocomputing 2015; 151: 139–50.

Leandrou S, Petroudi S, Kyriacou PA, Reyes-Aldasoro CC, Pattichis CS. Quantitative MRI brain studies in mild cognitive impairment and Alzheimer's disease: a methodological review. IEEE Rev Biomed Eng 2018; 11: 97–111.

LeCun Y, Bengio Y, Hinton G. Deep learning. Nature 2015; 521: 436–44.

Lee C, Zame WR, Yoon J, van der Schaar M. DeepHit: a deep learning approach to survival analysis with competing risks. In: Thirty-Second AAAI Conf Artif Intell; 2018.

Li Y, Jiang J, Shen T, Wu P, Zuo C. Radiomics features as predictors to distinguish fast and slow progression of mild cognitive impairment to Alzheimer's disease. Conf Proc IEEE Eng Med Biol Soc 2018; 2018: 127–30.

Liao L, Hyung-il A. Combining deep learning and survival analysis for asset health management. Int J Progn Heal Manag 2016; 7: 020.

Lin W, Tong T, Gao Q, Guo D, Du X, Yang Y, et al. Convolutional neural networks-based MRI image analysis for the Alzheimer's disease prediction from mild cognitive impairment. Front Neurosci 2018; 12: 777.

Luck M, Lodi A. Deep learning for patient-specific kidney graft survival analysis. arXiv:170510245v1 2017. Available at: http://medianetlab.ee.ucla.edu/papers/AAAI_2018_DeepHit.

Magnin B, Mesrob L, Kinkingnéhun S, Pélégrini-Issac M, Colliot O, Sarazin M, et al. Support vector machine-based classification of Alzheimer's disease from whole-brain anatomical MRI. Neuroradiology 2009; 51: 73–83.

Minkova L, Habich A, Peter J, Kaller CP, Eickhoff SB, Klöppel S. Gray matter asymmetries in aging and neurodegeneration: a review and meta-analysis. Hum Brain Mapp 2017; 38: 5890–904.

Montavon G, Lapuschkin S, Binder A, Samek W, Müller K-R. Explaining nonlinear classification decisions with deep Taylor decomposition. Pattern Recognit 2017; 65: 211–22.

Moradi E, Pepe A, Gaser C, Huttunen H, Tohka J. Alzheimer's Disease Neuroimaging Initiative. Machine learning framework for early MRI-based Alzheimer's conversion prediction in MCI subjects. Neuroimage 2015; 104: 398–412.

Mueller S, Keeser D, Reiser MF, Teipel S, Meindl T. Functional and structural MR imaging in neuropsychiatric disorders, Part 1: imaging techniques and their application in mild cognitive impairment and Alzheimer disease. AJNR Am J Neuroradiol 2012; 33: 1845–50.

Palop JJ, Mucke L. Amyloid-beta-induced neuronal dysfunction in Alzheimer's disease: from synapses toward neural networks. Nat Neurosci 2010; 13: 812–8.

Petersen RC, Roberts RO, Knopman DS, Boeve BF, Geda YE, Ivnik RJ, et al. Mild cognitive impairment: ten years later. Arch Neurol 2009; 66: 1447–55.

Ranganath R, Perotte A, Blei D. Deep survival analysis. Proc Mach Learn Healthc 2016; 56: 101–14.

Retico A, Bosco P, Cerello P, Fiorina E, Chincarini A, Fantacci ME. Predictive models based on support vector machines: whole-brain versus regional analysis of structural MRI in the Alzheimer's disease. J Neuroimaging 2015; 25: 552–63.

Seeley WW, Menon V, Schatzberg AF, Keller J, Glover GH, Kenna H, et al. Dissociable intrinsic connectivity networks for salience processing and executive control. J Neurosci 2007; 27: 2349–56.

Shen T, Jiang J, Li Y, Wu P, Zuo C, Yan Z. Decision supporting model for one-year conversion probability from MCI to AD using CNN and SVM. Conf Proc IEEE Eng Med Biol Soc 2018; 2018: 738–41.

Spasov S, Passamonti L, Duggento A, Liò P, Toschi N. Alzheimer's Disease Neuroimaging Initiative. A parameter-efficient deep learning approach to predict conversion from mild cognitive impairment to Alzheimer's disease. Neuroimage 2019; 189: 276–87.

Tondelli M, Wilcock GK, Nichelli P, De Jager CA, Jenkinson M, Zamboni G. Structural MRI changes detectable up to ten years before clinical Alzheimer's disease. Neurobiol Aging 2012; 33: 825.e25–36.

Zhang D, Shen D; Alzheimer's Disease Neuroimaging Initiative. Predicting future clinical changes of MCI patients using longitudinal and multimodal biomarkers. PLoS One 2012; 7: e33182.

Zhou H, Jiang J, Lu J, Wang M, Zhang H, Zuo C, et al. Dual-model radiomic biomarkers predict development of mild cognitive impairment progression to Alzheimer's disease. Front Neurosci 2019; 12: 1045.